Journal of
Engineering and
Applied Sciences

SINCE 2000
MEDWELL PUBLICATIONS

Double-Layer Coatings for Surface Improvement of Al 6061 Alloys by Anodizing and Micro Plasma Oxidation Process MPO using New Hydroxy Apatite and Rock Additives Modified Electrolytes

Samir Hamid Awad
Department of Ceramic and Building Materials, College of Materials Engineering, University of Babylon, P.O. Box:4, Hillah, Babylon, Iraq

Key words: Micro arc oxidation, Aluminium alloy, Rock additive, Hardness, wear resistance

Corresponding Author:
Samir Hamid Awad
Department of Ceramic and Building Materials, College of Materials Engineering, University of Babylon, P.O. Box:4, Hillah, Babylon, Iraq

Page No.: 3112-3121
Volume: 15, Issue 16, 2020
ISSN: 1816-949x
Journal of Engineering and Applied Sciences

Abstract: In this research, duplex ceramic coatings were deposited on Al 6061 alloy, using anodizing and Micro Plasma process (MPO). MPO electrolyte was modified using hydroxy apatite and 15 g L^{-1} rock additives rich with Calcium Carbonate (CaCo$_3$). Phase composition of the coatings, micro structure, micro-hardness, topography, thickness, roughness and wear resistance were evaluated by X-Ray Diffraction (XRD), (SEM), a Vickers indenter, AFM and Microprocessor coating thickness meter, roughness test and Micro test, respectively. Results showed that the samples coatings contained γ-alumina and their thickness and hardness increased by the increasing of deposition time. The research demonstrates that a relatively hard, thick and uniform coatings with good wear resistance, can successfully be deposited on Al alloy using hydroxy apatite and 15 g L^{-1} CaCo$_3$ rock additives containing electrolytes as an natural rock additives.

INTRODUCTION

The treatments for surface improvement of Al alloys such as chemical conversion coatings, anodic oxidation, laser processing and ion implantation ,are increasingly used to modify their surface for heavy load bearing applications[1]. MAO process is a new effective surface treatment technique to enhance the tribological properties of Al alloys by deposition of hard and thick alumina coatings[2-9]. Many studies have been done on the modification of the electrolytes by using multiple additives (micro and nano additive), to improve the coatings mechanical and tribological properties[10-14]. The MAO oxidation method is a combination of plasma discharge and anodizing oxidation and the initially of the MAO method is an anodization method[15]. In anodizing, durable and porous coatings are formed by oxidation and durable surface coating to improve the corrosion resistance of Al surfaces[16-18]. Anodizing is a widely used process which is distinctive by the good appearance and lower energy depreciation. However, the anodization porous oxide films cannot have satisfied hardness and anti corrosion performance[1].

In our study, anodic and MAO duplex coatings were combined to get their advantages. Also, this study is an attempt in using of Iraqi rock additives rich with Calcium Carbonate (CaCo$_3$) with nano hydroxy apatite in modification the MAO electrolyte as an assistant additives for surface modification of pre-anodized Al alloys. Iraqi land is rich of rock materials that contain natural materials like $CaCO_3$. $CaCO_3$ is white, fine and odourless powder. $CaCO_3$ is one of the most plentiful materials found in earth’s crust and forms the rock sorts like chalk and limestone[19].

MATERIALS AND METHODS

Experimental

Powder preparation; Preparation of nano HA powder: The wet chemical precipitation process was used for preparation of nano HA powder using chemical precipitation process using precursors of $(NH_4)_2\ HPO_4$ and $Ca(NO_3)_2\ 4H_2O$ and NH_2OH as the precipitant. XRD and particle size tests were conducted to identify the powder and to characterize particle size. The test results proved pure hexagonal Hydroxy apatite $Ca_{10}(PO_4)_6\ (OH)_2$ powder with particle size of 250 nm because of the high agglomerations occur due to the surface area of the particles.

Preparation of calcite powder: In this process, a suitable amount of calcium carbonate rocks was selected from (lime factory, Karbala/Iraq) and manually kibbled using mortar to get the quasi-finished powder. Then the powder was milled for 5 h by using ball mill at speed 350 rpm. After milling, powder was tested by laser particle size analyzer (Type Better size 2000) and XRD. The test results proved pure $CaCO_3$ powder with particle size of about (3 µm).

Samples preparation: Samples from Al 6061 alloy with hardness of 75HV were cut into dimensions of ($\varphi 25\times 5\ mm^2$). The chemical composition of Al substrates is given in Table 1. All samples were polished to get surface roughness Ra = 0.1 µm, before anodization, then they were dipped into methanol and ultrasonic vibration. After that the samples were immersed in 5 mass% NaOH alkaline solution at 60°C for 45 sec for degreasing and water rinsed for 15 min. In the pickling process, samples were submerged for 60 sat room temperature in 30 vol% HNO_3 aqueous solution followed by water rinsing 15 min (Table 1).

Anodizing and micro arc oxidation process: The anodization was conducted at 15 V constant voltage and 15 mA cm^{-2} at 15°C for12 min in a 15 wt.% H_2SO_4 solution. The anodized samples were sealed in hot waterfor15 min at 95°C. A500VDC-AC homemade MAO deposition unit shown in Fig. 1 was used to deposit the ceramic coatings at fixed current density of (5) A dm^{-2} and voltage of 380 V. A five litters bath from container was used. In the plastic container, the electrolyte was agitated and cooled using a mechanical stirrer and cooling system, respectively. Also, the plastic container was equipped with a sample holder as the anode and a st st 316L plate serving as the cathode. The cooling unit connected to the MAO unit works to prevent electrolyte solution heating over to 30°C. It provides the cooled water to a big plastic container surrounded the electrolyte solution container. Then, all samples were rinsed in distilled water and, dried in air.

Table 1: Al 6061 alloy chemical composition

Elements	Content (wt.%)	Elements	Content (wt.%)
Si	0.50	Zn	0.1
Fe	0.30	Cr	0.2
Cu	0.10	Other	0.12
Mn	0.10	Al	Bal.
Mg	0.79		

The electrolytic solutions were mixed after preparation for 2 h before the MAO process. Table 2 and 3 show the electrolyte composition and deposition parameters.

Characterization: The powders and substrates were identified using X-ray Diffractometer (XRD-6000SHIMADZU, Japan, Cu Kα radiation, 40 kV, 30MA, 6°/min scanning speed). The coatings were tested with XRD-7000 SHIMADZU system. The micro structure was studied using scanning electron microscope (INSPECT S50, FEI Company). Micro-hardness was measured by a Vickers indenter (HVS-1000, Laryee,

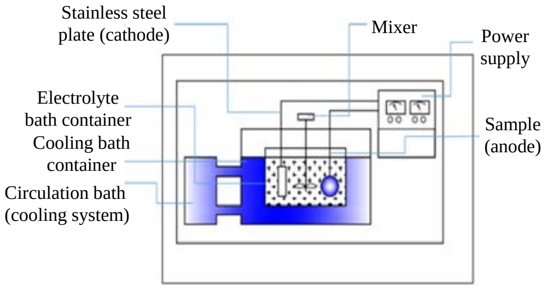

Fig. 1: MAO coating equipment

Table 2: Composition of modified electrolytes

Component	Concentration (g L^{-1})	Specification
KOH	3	Electrolyte conductivity increasing
$KH_2\ PO_4$	15	Property modification
HA	20	Assistance
$CaCO_3$	15	Assistance

Table 3: Deposition parameters

Sample code	Deposition time (min)
ME_1	10
ME_2	20
ME_3	40
ME_4	60

digital Micro-hardness tester) with load of 4.9 N and holding time of 15 sec. Microprocessor CM-8822, coating thickness was employed to measure thickness coatings. All experimental measurements of 3D surface topography and roughness parameters were obtained using Atomic Force Microscopy (AFM, contact mode, spm AA3000 Angstrom advanced Inc., USA), prior to AFM analysis the surface of the samples was cleaned with alcohol and dried at room temperature. The wear resistance was tested using (Microtest-28021) and 6 mm carbide pin at load 10 N, sliding speed 200 rpm, sliding distance 75 mm and time 15 min.

RESULTS AND DISCUSSION

MAO spark conditions: The recorded values for the voltage-current during the MAO treatment using the natural additives containing electrolytes could clearly show the normal and continuous sparks movement at 380 V and 5 A dm^{-2} current density. The spark movement can be attributed to the deposition of substrate and spot localized healing with the subsequent sparking at weak spots in the coating. Anyhow, raising the voltage above 280 V could start the dielectric breakdown and it varied with the anode material and the electrolyte temperature and composition.

XRD results: Figure 2 and 3, display the XRD results of the coated samples. XRD patterns proved the deposition of aluminum oxide on the surface of substrates. The mean peaks were γ-Al_2O_3(JCPDS No. 010-0425). The Al peaks (JCPDS No. 004-0787) observed in XRD results can be attributed to the thicknesses and Al peaks coming from the underlying substrate were detected due to the X-rays penetration into the Al substrates. Typically, it could be observed that at high Bragg angels the thin films have low intensities[12].

EDS results: Figure 4-7 show the results of EDS. The EDS results could indicate the deposition of aluminum oxide. The existence of Aluminum (Al) and Oxygen (O) elements in the coatings, referred to the Al_2O_3 layers formation with different weights of modification elements of C, P, Ca, Si and Na. Generally, Celement is always precipitated in the MAO electrolytes, deposited as contaminate and detected on the unpolished coatings. Furthermore, other elements may be resulted from the contaminates in hydroxy apatite and $CaCO_3$ .Also, P is belonged to the chemical compounds used in preparation of the electrolytes .Generally, different elements used in preparation of electrolytes could react with Al of substrate

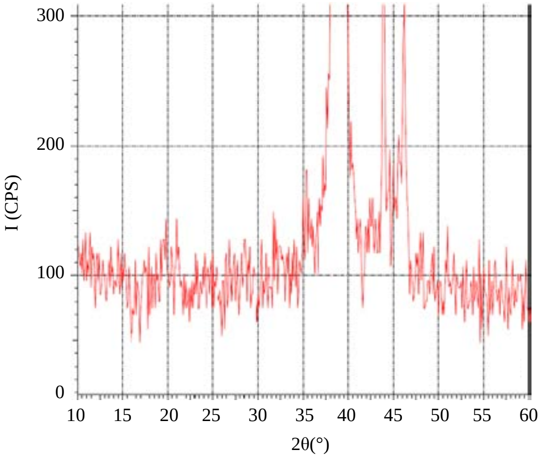

Fig. 2: XRD patterns of sample ME_1

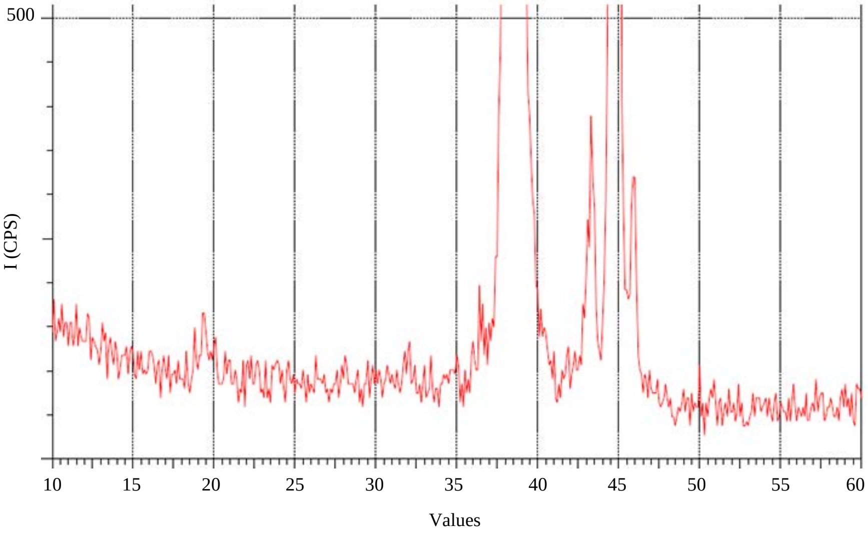

Fig. 3: XRD patterns of sample ME_4

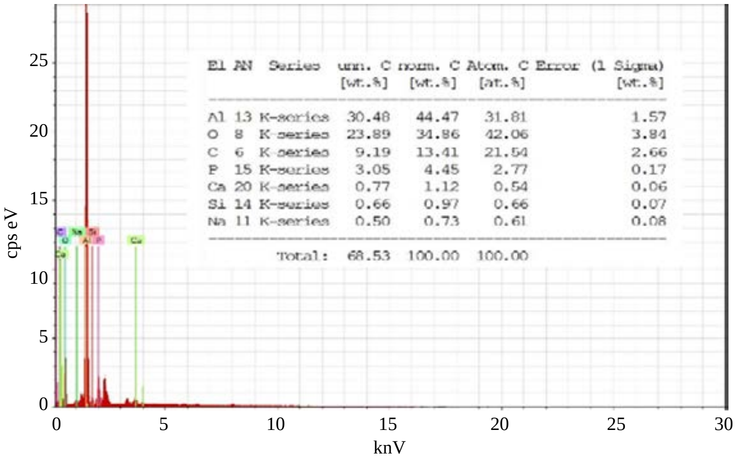

```
El AN  Series   unn. C norm. C Atom. C Error (1 Sigma)
                [wt.%]  [wt.%]  [at.%]          [wt.%]
-------------------------------------------------------
Al 13 K-series  30.48   44.47   31.81            1.57
O   8 K-series  23.89   34.86   42.06            3.84
C   6 K-series   9.19   13.41   21.54            2.66
P  15 K-series   3.05    4.45    2.77            0.17
Ca 20 K-series   0.77    1.12    0.54            0.06
Si 14 K-series   0.66    0.97    0.66            0.07
Na 11 K-series   0.50    0.73    0.61            0.08
-------------------------------------------------------
        Total:  68.53  100.00  100.00
```

Fig. 4: EDS of sample ME_1

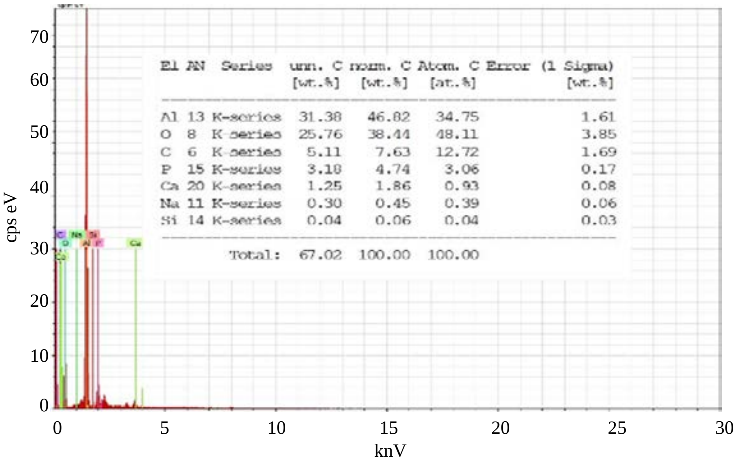

```
El AN  Series   unn. C norm. C Atom. C Error (1 Sigma)
                [wt.%]  [wt.%]  [at.%]          [wt.%]
-------------------------------------------------------
Al 13 K-series  31.38   46.82   34.75            1.61
O   8 K-series  25.76   38.44   48.11            3.85
C   6 K-series   5.11    7.63   12.72            1.69
P  15 K-series   3.18    4.74    3.06            0.17
Ca 20 K-series   1.25    1.86    0.93            0.08
Na 11 K-series   0.30    0.45    0.39            0.06
Si 14 K-series   0.04    0.06    0.04            0.03
-------------------------------------------------------
        Total:  67.02  100.00  100.00
```

Fig. 5: EDS of sample ME_2

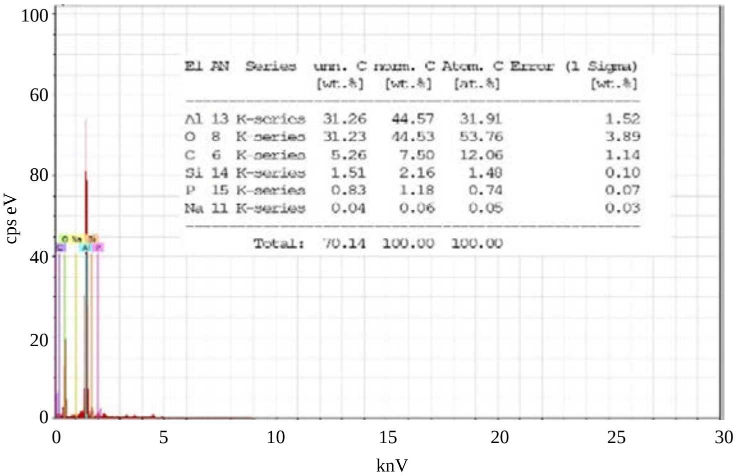

```
El AN  Series   unn. C norm. C Atom. C Error (1 Sigma)
                [wt.%]  [wt.%]  [at.%]          [wt.%]
-------------------------------------------------------
Al 13 K-series  31.26   44.57   31.91            1.52
O   8 K-series  31.23   44.53   53.76            3.89
C   6 K-series   5.26    7.50   12.06            1.14
Si 14 K-series   1.51    2.16    1.48            0.10
P  15 K-series   0.83    1.18    0.74            0.07
Na 11 K-series   0.04    0.06    0.05            0.03
-------------------------------------------------------
        Total:  70.14  100.00  100.00
```

Fig. 6: EDS of sample ME_3

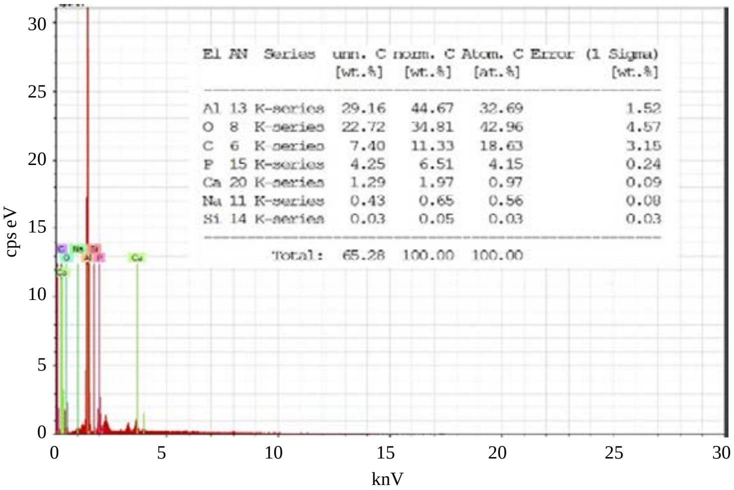

El	AN	Series	unn. C [wt.%]	norm. C [wt.%]	Atom. C [at.%]	Error (1 Sigma) [wt.%]
Al	13	K-series	29.16	44.67	32.69	1.52
O	8	K-series	22.72	34.81	42.96	4.57
C	6	K-series	7.40	11.33	18.63	3.15
P	15	K-series	4.25	6.51	4.15	0.24
Ca	20	K-series	1.29	1.97	0.97	0.09
Na	11	K-series	0.43	0.65	0.56	0.08
Si	14	K-series	0.03	0.05	0.03	0.03
		Total:	65.28	100.00	100.00	

Fig. 7: EDS of sample ME_4

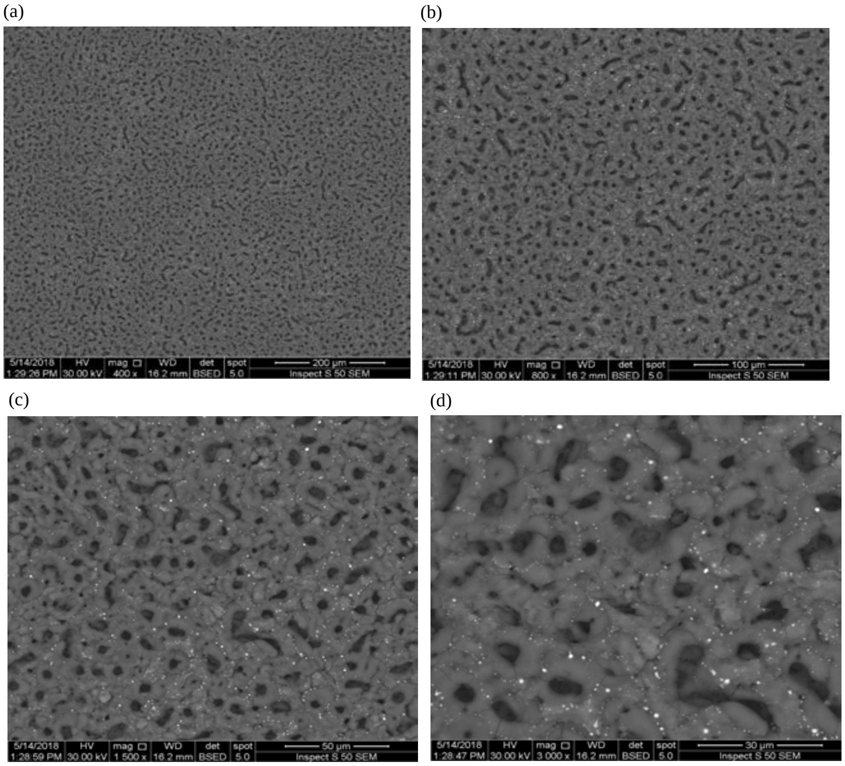

Fig. 8(a-d): Surface morphology results from SEM observation of sample ME_1 at different magnifications

to produce complex compounds, may also be alloyed within the MAO sparks, leading to the high content of such elements on the deposited coatings.

Sem results: Figure 8-11 show the surface morphology results from SEM for the coated sample at different magnifications. The morphologies can be observed are characterized by different sizes of sphere-like geometry pores in the structure. These coatings have a pan-like structures with a non-uniformly distributed porous structures. At the discharge spots sites, the metal from substrate and its oxide are melted and projectile over from discharge tunnels due to the very high temperatures at those sites. The observed pan-cake-like morphologyis resulted from the molten liquid that quickly solidified leaving distinct boundaries around the pores. Also such rapid solidification induced the microcracks appearance on the morphology due to molten oxide continuous exposing to cold electrolyte. In general, sample ME_2 (at 20 min) showed structure characterized by pores non-uniform distribution and their different sizes. Considering such non-uniform distribution of porosity, it could have its effects in lowering the hardness of sample ME_2 in comparison with other samples. In general, the hardness differences is strongly attributed to the non-uniform distribution of pores in coatings. The MAO discharge canals can result in a highly thick and porous films and the components and any modifying elements in

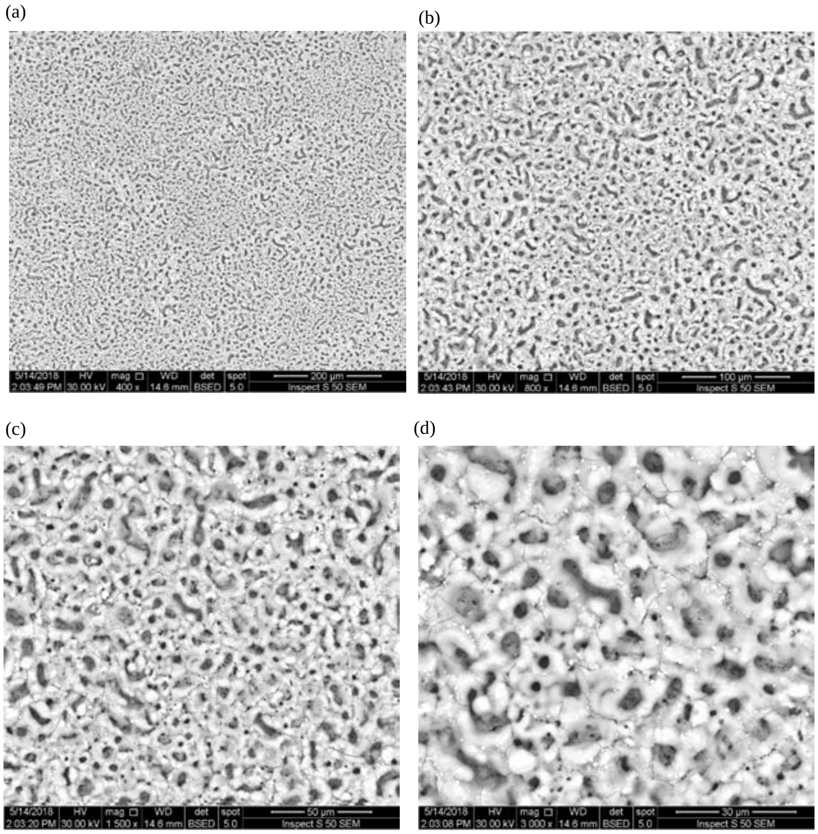

Fig. 9(a-d): Surface morphology results from SEM observation of sample ME_2 at different magnifications

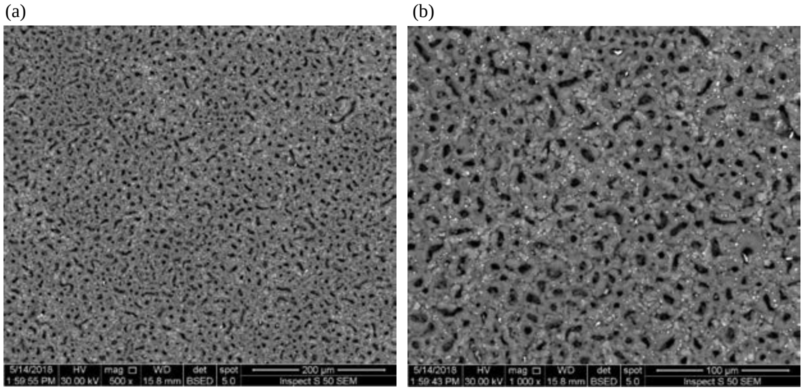

Fig. 10(a-d): Continue

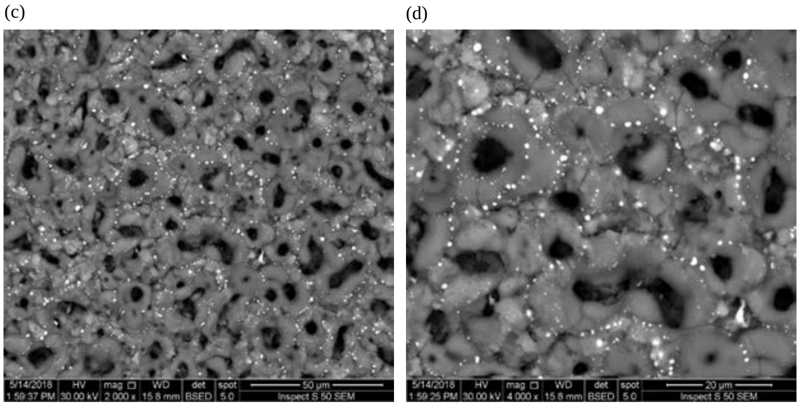

Fig. 10(a-d): Surface morphology results from SEM observation of sample ME_3 at different magnifications

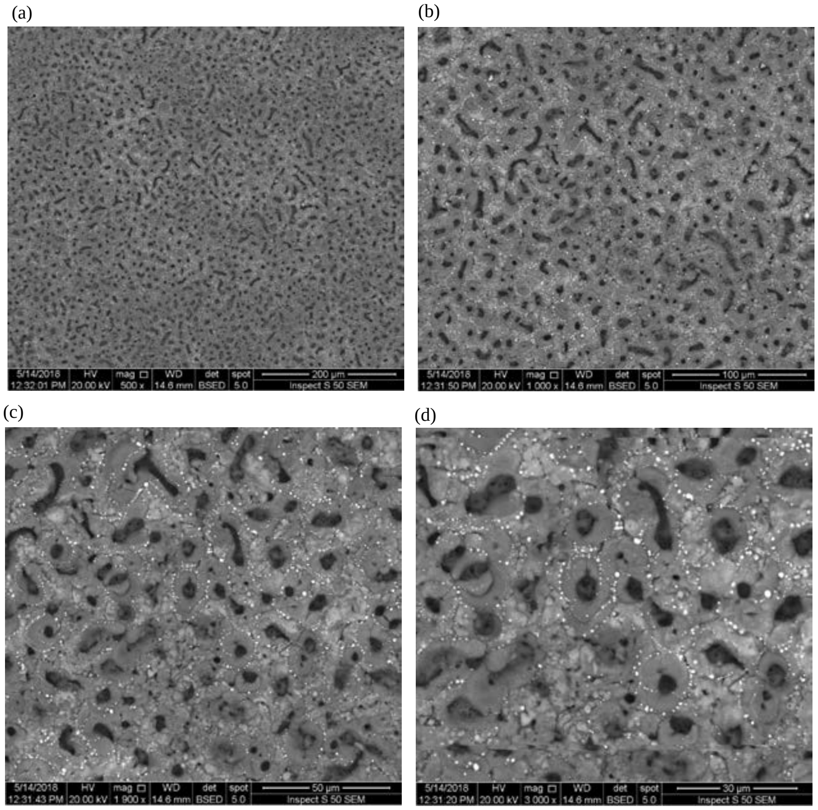

Fig. 11(a, b): Surface morphology results from SEM observation of sample ME_4 at different magnifications

the electrolytes can be incorporated into oxide films by the discharge. The structure of ME_4 was characterized by relatively low pores with uniform distribution which has its effects on the increasing hardness values.

Thickness and Hardness results of coatings: The pre anodized treatment could provide 10-13 µm ceramic coatings with hardness of 200 Hv. Table 4 presents the results from thickness and hardness. Figure 12-14 give the effect of deposition time on the resulted hardness and coatings thickness with and without pre treatment. In general, double-layer coatings deposited by anodizing and process MPO processes using new hydroxy apatite and $CaCo_3$ rock additives modified electrolytes could improve the Al substrates with thick and hard ceramic alumina in comparison to untreated coatings. Anodizing permanently changes the outer structure of the oxidized surface and make it much thicker, up to several

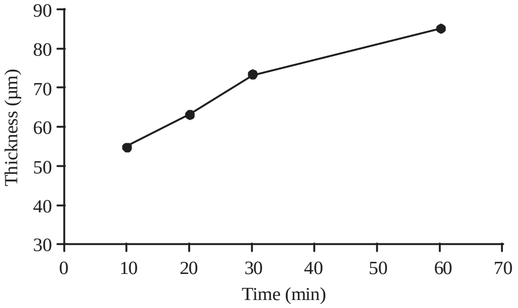

Fig. 12: Effect of deposition time on coatings thickness

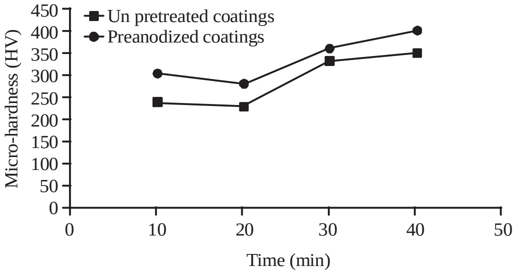

Fig. 13: Effect of deposition time on coatings hardness

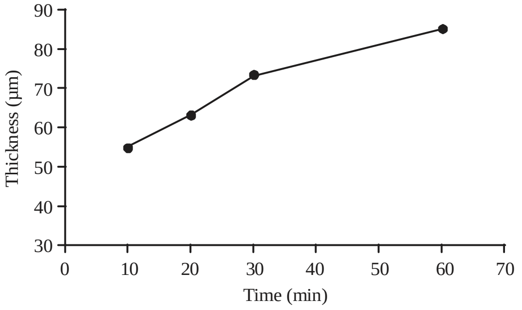

Fig. 14: Effect of deposition time on coatings roughness

Table 4: Wear results

Samples	Weight loss (g)
Substrate	42×10^{-4}
ME_1	10×10^{-4}
ME_2	8×10^{-4}
ME_3	7×10^{-4}
ME_4	5×10^{-4}

micrometers. The anodized aluminum oxide coating is very hard, The porous nature of oxidized surface makes it possible to impregnate such pores with the number of discrete short-lived micro discharges moving across the Al surface during the subsequent MAO process. The variation of coatings thickness with deposition time can be attributed to the broken of weak oxide layer by strong spark during growth, thereby, forms different thickness values. It can be concluded that the thickness values were (55-85) µm and the sample ME_4 exhibited the highest value (85 µm) at 60 min in comparison with the other coatings. While sample ME_1 recorded the lowest (55 µm) thickness at 10 min. Generally, the increasing of coating thickness can be observed with deposition time increasing. It is interested to mention that, only the micro-hardness test at 4.9 N and holding time (15 sec) could evaluated the coating hardness. In general using loads of 50, 100, 150, 250, 350,400 g could not show any track in the coating surface. The dense layer exhibited the higher value of hardness while the hardness of porous layer was rather low. It can be observed that, the sample ME_2 recorded the lowest (230-280 HV) hardness because of their porous structures characterized by more nonuniform pores distribution in ceramic oxide pointed in SEM results. The ceramic coatings showed surface roughness in the range (1.72-16.5) µm. Generally, the coating roughness decreased with deposition time increasing.

Table 5: Results of coatings thickness and hardness and roughness

Sample	Thickness (µm)	Hardness (HV) Un pretreated	 Preanodized	Roughness (µm)
ME_1	55	239	300	11.60
ME_2	63	230	280	6.80
ME_3	73	329	360	1.72
ME_4	85	350	400	16.50

AFM results: The surface roughness of each sample is measured along the same reference length, what can be seen on the 2D view of Fig. 15. The obtained results of the coatings are presented in the form of high resolution 3D images. The measurement range on all samples is 4000×4000 nm. Figure 15 shows 3D topographies and roughness profiles of the coatings. From presented results of AFM in Fig. 14 and 15, it can be said that the ceramic coatings showed surface roughness in the range (1.72-16.5) µm. Generally, the coating roughness decreased with deposition time increasing to 30 min, then the coatings of sample ME_4 have surface roughness higher those of other samples due to increasing of coating thickness. Anyhow, AFM results showed cluster of particles with highly dense structure, the particles were closely bonded and no voids were observed in samples. While the voids were appeared in sample ME_4 which indicated that the surface roughness increased with the increasing of deposition time to 60 min.

Wear results: The wear mass loss of test samples weighted to an accuracy of 0.1 mg produced by pin-on disc sliding wear test were used to evaluate the wear rate. The values of weight loss are shown in Table 5. The Al substrate had a higher weight loss of 42×10^{-4} g while samples coated using modified electrolytes had weight loss of 5×10^{-4}-10×10^{-4} g. Such results could prove the

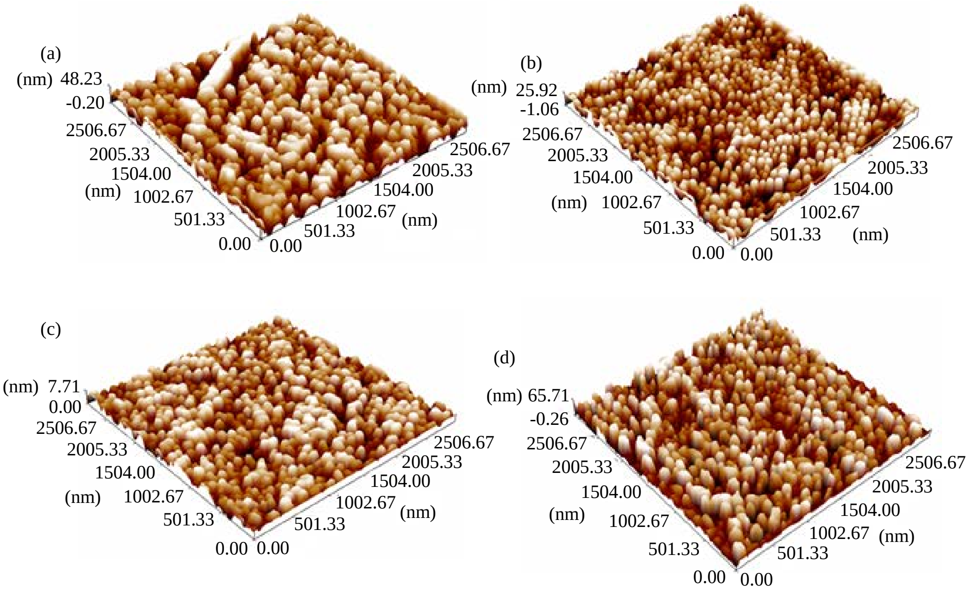

Fig. 15(a, b): AFM Results of samples ME, (a) Ra = 11.6, 10 min, (b) Ra = 6.8, 20 min, (c) Ra = 1.72 40 min and (d) Ra = 16.5, 60 min

successes of the pretreatment of anodizing and the using of new hydroxy apatite and rock additives modified electrolytes for surface improvement of Al alloys to deposit oxide layers with good wear resistance.

CONCLUSION

The pretreatment of anodizing and using of new MAO electrolytes modified by nano hydroxy apatite and CaCo$_3$ natural rock additives can be used to deposit hard and thick γ-Al$_2$O$_3$ coatings on Al alloy substrates. The MAO ceramic coatings with thicknesses (55-85) µm can enhance the Al hardness from (75)-(280-400) HV. Hardness differences were strongly affected by the non-uniform distribution of pores and increased with increasing of deposition time. The micro structure of coatings was characterized by different size of pores and distributions. The AFM results showed an average roughness in the range (1.72-16.5 µm) which decreased with increasing of deposition time to 40 min, then showed maximum value at 60 min due to the highest coating thickness. The wear resistance improved by MAO coatings using the modified electrolyte and the weight loss decreased from 42×10^{-4} for Al alloy to 5×10^{-4} for thick ceramic coatings deposited for 60 min.

REFERENCES

01. Zhao, X., D. Liu, J. Lu and G. Wei, 2017. Micro-arc oxidation coating formed on anodized Aluminum surface under different pulse frequencies. Intl. J. Electrochem. Sci., 12: 7922-7930.

02. Clyne, T.W. and S.C. Troughton, 2019. A review of recent work on discharge characteristics during plasma electrolytic oxidation of various metals. Intl. Mater. Rev., 64: 127-162.

03. Zhang, Y., Y. Chen, H.Q. Du and Y.W Zhao, 2018. Corrosion resistance of micro-arc oxidation coatings formed on Aluminum alloy with addition of Al$_2$O$_3$. Mater. Res. Express, 5: 036527-036527.

04. Yang, W., W. Liu, Z. Peng, B. Liu and J. Liang, 2017. Characterization of plasma electrolytic oxidation coating on low Carbon steel prepared from silicate electrolyte with Al nanoparticles. Ceram. Intl., 43: 16851-16858.

05. Lederer, S., P. Lutz and W. Furbeth, 2018. Surface modification of Ti 13Nb 13Zr by plasma electrolytic oxidation. Surf. Coat. Technol., 335: 62-71.

06. Sobolev, A., A. Kossenko, M. Zinigrad and K. Borodianskiy, 2018. Comparison of plasma electrolytic oxidation coatings on Al alloy created in aqueous solution and molten salt electrolytes. Surf. Coat. Technol., 344: 590-595.

07. Zhang, Y., W. Fan, H.Q. Du and Y.W. Zhao, 2017. Corrosion behavior and structure of plasma electrolytic oxidation coated Aluminum alloy. Intl. J. Electrochem. Sci., 12: 6788-6800.

08. Li, H. and J. Zhang, 2017. Preparation of a modified Micro-arc oxidation coating using Al$_2$O$_3$ particles on Ti-6Al-4V. J. Mater. Sci. Eng., 6: 1-6.

09. Malyshev, V.N. and A.M. Volkhin, 2013. Antifriction properties increasing of ceramic MAO-coatings. Proc. Inst. Mech. Engi. Part J. J. Eng. Tribol., 228: 435-444.
10. Vatan, H.N., R.E. Kahrizsangi and M.K. Asgarani, 2016. Effect of WC nano-powder on properties of plasma electrolytic oxidation coating fabricated on AZ31B Alloy. Intl. J. Electrochem. Sci., 11: 929-943.
11. Daroonparvar, M., M.A.M. Yajid, N.M. Yusof and H.R. Bakhsheshi-Rad, 2016. Preparation and corrosion resistance of a nanocomposite plasma electrolytic oxidation coating on Mg-1% Ca alloy formed in Aluminate electrolyte containing Titania nano-additives. J. Alloys Compd., 688: 841-857.
12. Kiselyeva, S.K., L.I. Zaynullina, M.M. Abramova, N.Y. Dudareva and I.V. Alexandrov, 2014. The effect of Microarc Oxidation (MAO) modes on corrosion behavior of high-silicon Aluminum alloy. J. Eng. Sci. Technol. Rev., 7: 36-39.
13. Ding, H.Y., Z.D. Dai, S.C. Skuiry and D. Hui, 2010. Corrosion wear behaviors of micro-arc oxidation coating of Al_2O_3 on 2024Al in different aqueous environments at fretting contact. Tribol. Int., 43: 868-875.
14. Pezzato, L., V. Angelini, K. Brunelli, C. Martini and M. Dabala, 2018. Tribological and corrosion behavior of PEO coatings with graphite nanoparticles on AZ91 and AZ80 magnesium alloys. Trans. Nonferrous Met. Soc. China, 28: 259-272.
15. Hussein, R.O. and D.O. Northwood, 2014. Production of Anti-Corrosion Coatings on Light Alloys (Al, Mg, Ti) by Plasma-Electrolytic Oxidation (PEO). In: Developments in Corrosion Protection, Aliofkhazraei, M. (Ed.). IntechOpen, England, UK., ISBN:978-953-51-1223-5, pp: 201-240.
16. Labisz, K., J. Konieczny, L. Wierzbicki, J. Cwiek and A. Butor, 2018. Influence of primary Silicon precipitates on anodized Aluminum alloys surface layer properties. Transp. Prob., 13: 111-120.
17. Ajeel, S.A., N.W. Kasser and B.A. Abdul-Hussein, 2010. Breakdown and pitting formation of anodic film Aluminum alloy (3003). Mod. Appl. Sci., 4: 87-101.
18. Shih, T.S., T.H. Lee and Y.J. Jhou, 2014. The effects of anodization treatment on the microstructure and fatigue behavior of 7075-T73 Aluminum alloy. Mater. Trans., 55: 1280-1285.
19. Al Omari, M.M.H., I.S. Rashid, N.A. Qinna, A.M. Jaber and A.A. Badwan, 2016. Calcium Carbonate. In: Profiles of Drug Substances, Excipients and Related Methodology, Brittain, H.G. (Ed.). Academic Press, Cambridge, Massachusetts, USA., pp: 31-132.